Santa Clara University
Scholar Commons

Civil Engineering   School of Engineering

11-2002

A Long-Term Hydrologically-Based Data Set of Land Surface Fluxes and States for the Conterminous United States

Edwin P. Maurer
Santa Clara University, emaurer@scu.edu

A. W. Wood

J. C. Adam

Dennis P. Lettenmaier

B. Nijssen

Follow this and additional works at: https://scholarcommons.scu.edu/ceng

Part of the Civil and Environmental Engineering Commons

A Long-Term Hydrologically Based Dataset of Land Surface Fluxes and States for the Conterminous United States*

E. P. Maurer, A. W. Wood, J. C. Adam, and D. P. Lettenmaier

Department of Civil and Environmental Engineering, University of Washington, Seattle, Washington

B. Nijssen

*Departments of Civil Engineering and Engineering Mechanics and Hydrology and Water Resources,
University of Arizona, Tucson, Arizona*

ABSTRACT

A frequently encountered difficulty in assessing model-predicted land–atmosphere exchanges of moisture and energy is the absence of comprehensive observations to which model predictions can be compared at the spatial and temporal resolutions at which the models operate. Various methods have been used to evaluate the land surface schemes in coupled models, including comparisons of model-predicted evapotranspiration with values derived from atmospheric water balances, comparison of model-predicted energy and radiative fluxes with tower measurements during periods of intensive observations, comparison of model-predicted runoff with observed streamflow, and comparison of model predictions of soil moisture with spatial averages of point observations. While these approaches have provided useful model diagnostic information, the observation-based products used in the comparisons typically are inconsistent with the model variables with which they are compared—for example, observations are for points or areas much smaller than the model spatial resolution, comparisons are restricted to temporal averages, or the spatial scale is large compared to that resolved by the model. Furthermore, none of the datasets available at present allow an evaluation of the interaction of the water balance components over large regions for long periods. In this study, a model-derived dataset of land surface states and fluxes is presented for the conterminous United States and portions of Canada and Mexico. The dataset spans the period 1950–2000, and is at a 3-h time step with a spatial resolution of ⅛ degree. The data are distinct from reanalysis products in that precipitation is a gridded product derived directly from observations, and both the land surface water and energy budgets balance at every time step. The surface forcings include precipitation and air temperature (both gridded from observations), and derived downward solar and longwave radiation, vapor pressure deficit, and wind. Simulated runoff is shown to match observations quite well over large river basins. On this basis, and given the physically based model parameterizations, it is argued that other terms in the surface water balance (e.g., soil moisture and evapotranspiration) are well represented, at least for the purposes of diagnostic studies such as those in which atmospheric model reanalysis products have been widely used. These characteristics make this dataset useful for a variety of studies, especially where ground observations are lacking.

1. Introduction

Early evidence of the importance of the land surface as a boundary condition in climate modeling (Namias 1952, 1962) helped inspire the incorporation of land surface representations in coupled atmospheric models (Manabe 1969). As computational capabilities have improved, the representations of the land surface included in these coupled models have become more detailed (e.g., Mahrt and Pan 1984). Investigations using coupled land–atmosphere models have shown significant sensitivity of precipitation forecasts for lead times of several days to initial land surface states such as soil moisture (Beljaars et al. 1996; Betts et al. 1996a), and to long-lead (months or more) forecasts of surface air temperature (Huang et al. 1996). These sensitivities, of course, vary regionally and seasonally. For example, Brubaker et al. (1993) argue that precipitation forecasts should be most sensitive to land surface conditions where local feedbacks exist through recycling of moisture via evapotranspiration,

---

Corresponding author address: Dennis P. Lettenmaier, Department of Civil and Environmental Engineering, University of Washington, P.O. Box 352700, Seattle, WA 98195-2700.
E-mail: lettenma@ce.washington.edu

which in general suggests that sensitivities should be highest in midcontinental areas in summer. This has been confirmed recently in experiments by Koster et al. (2000), where soil moisture memory was shown to be a dominant source of long-term weather predictability for some mid-latitude continental regions.

The greatest difficulty in assessing the performance of coupled (and uncoupled) land–atmosphere parameterizations is the absence of comprehensive land surface observations against which simulations can be compared at the spatial and temporal resolutions at which the models operate. The Atmospheric Model Intercomparison Project (Gates 1992) included global climate simulations using 31 different coupled models, producing output including land surface variables of soil moisture, snow, and latent and sensible heat fluxes. In the validation stage, Gates et al. (1999) compare modeled precipitation to a gridded global dataset based on both gauge and satellite estimates (Xie and Arkin 1997), while most remaining surface variables were only intercompared, due to the limited quality and coverage of observations. Several methods have been used to evaluate the land surface representations in coupled models in so-called off-line experiments, that is, where surface forcings to the models (precipitation, surface air temperature, as well as other surface meteorological variables and radiative forcings) are prescribed. These include comparisons of model-predicted evapotranspiration with those derived from an atmospheric water balance (Lohmann et al. 1998a), comparison of model-predicted energy and radiative fluxes with tower measurements during periods of intensive observations (Betts et al. 1996b), comparison of model-predicted runoff with observed streamflow (Koster et al. 1999), and comparison of model predictions of soil moisture with spatial averages over large regions of point observations of soil moisture (Robock et al. 1998). While these approaches have provided useful model diagnostic information, the observation-based products used in the comparisons in all cases have some inconsistency with the model variables with which they are compared—for example, observations are for points or areas much smaller than the model spatial resolution (in the case of tower observations), comparisons are restricted to temporal averages rather than time step evolution of predicted variables (in the case of soil moisture), or the spatial scale is large compared to that resolved by the model (in the case of estimates of evapotranspiration based on atmospheric budget analysis). Furthermore, none of the datasets available at present allows an evaluation of the interaction of the water balance components over large regions for long periods.

A recent report of the U.S. Global Change Research Program (Hornberger et al. 2001) on global water cycle research identified as one of its three "pillar initiatives" determination of "whether or not the global water cycle is intensifying and to what degree human activities are responsible." A key element in any attempt to identify possible ongoing changes in the land surface component of the global water cycle is the use of long records to determine the variability of land surface moisture fluxes and storages. The lack of long-term, continent-wide observations of many of the component variables of the water cycle greatly complicates the direct determination of changes in most of these variables (Ziegler et al. 2002).

Global reanalyses, such as those produced using global forecast models of the U.S. National Centers for Environmental Prediction (NCEP; Kalnay et al. 1996) and the European Centre for Medium-Range Weather Forecasts (Gibson et al. 1997) provide one means of diagnosing model predictions of moisture and energy fluxes in the atmosphere and at the land surface. The reanalyses are produced by implementing a fixed or "frozen" version of a weather forecast model retrospectively, using the best available data in the analysis cycle, and archiving the model analysis output, which forms a consistent space–time field of all fluxes and state variables simulated by the model. The initial reanalysis produced using the NCEP model [produced in cooperation with the National Center for Atmospheric Research (NCAR), and usually referred to as the NCEP–NCAR reanalysis] is termed NRA1, to distinguish it from a more recent reanalysis, referred to here as NRA2, that uses the same forecast model (Ebisuzaki et al. 1998; Kanamitsu et al. 2000). NRA1 has been widely used for moisture and energy budget studies, model diagnosis, and many other purposes where temporally and spatially continuous/discrete fields are needed. E. Kalnay (2001, personal communication) and her colleagues estimate that over 3000 journal articles have made use of NRA1 directly or indirectly in the 5 years since the data (now periodically updated to cover the more than 50-yr period from 1949 to within approximately one month of current time) were first made publicly available. Reanalyses like NRA1 and NRA2 can provide an excellent resource for studies examining variables that are closely linked to assimilated variables (mostly atmospheric profiles of moisture, temperature, and wind), and in fact Kalnay et al. (1996) provide a classification of the quality of NRA1 variables that is largely based on how closely related an archived variable is to assimilated observations. Under this scheme, variables related to the land surface water budget are assigned to class C, meaning there are no observations directly affecting the variables, which are completely determined by the model, and may have considerable biases. For example, large biases have been identified in NRA1 precipitation (Higgins et al. 1996; Janowiak et al. 1998; Trenberth and Guillemot 1998), evapotranspiration (Lenters et al. 2000), runoff (Roads and Betts 2000; Coe 2000), snow and soil moisture (Lenters et al. 2000; Maurer et al. 2001), although interannual variability of some variables, such as precipitation and runoff have been found to be better simulated (Roads and Betts 2000). The follow-up NRA2 dataset reduces NRA1 land surface water budget biases, though

some biases remain (Maurer et al. 2001), and NRA2 covers a much shorter period, covering the "satellite" era of 1979–2000.

A major cause of problems with land surface variables in both NRA1 and NRA2 is the use of soil moisture "nudging" (or adjustment in the case of NRA2), which results in nonclosure of the surface water budget. Maurer et al. (2001) showed that the nonclosure term can be of the same order as other terms (e.g., runoff) in the surface water cycle. Although nudging in a reanalysis is designed to bring the model state (especially atmospheric moisture variables) closer to observations, this is done at the expense of other components of the water budget, and complicates studies focused on the interaction and variability of water budget components at the land surface [see, e.g., Maurer et al. (2001) for an assessment of the effect of soil moisture nudging on runoff in NRA1]. For these reasons, reanalysis data can be inappropriate for diagnosis of land surface moisture and energy flux and state variable simulations, by either uncoupled or coupled land–atmosphere models (Maurer et al. 2000), especially where the relationships between the budget components and their variability are of interest.

As argued by Maurer et al. (2000, 2001), better data for diagnosis of land surface water budget simulations can be produced through use of a physically based land surface model forced with quality controlled surface variables, and whose predicted surface runoff, when routed to correspond to streamflow measurements at the outlet of large river basins, matches observations. The effective degrees of freedom in a land surface scheme can be greatly reduced by prescribing, rather than predicting, model forcing variables at the land surface. For consistency of results, land surface schemes should, by construct, close the surface water and energy budgets (Pitman et al. 1999), and given the closure of these budgets by design, the variability and interaction of other "internal" variables can be expected to be much more realistic than those produced by reanalyses (or for that matter, any coupled model) that include some type of updating of model states.

We describe in this paper a consistent set of observation-based land surface forcings, and derived surface fluxes and state variables for a 50-yr period that is more or less consistent with that available from NRA1. Like the reanalyses, the derived data are based on use of a consistent model for the entire simulation period and model domain. The time step is subdaily (3 h), and the model (and hence derived data) spatial resolution is ⅛°. The domain covers all of the conterminous United States plus a bounding area that covers parts of Canada and Mexico (specifically latitudes 25°–53°N and longitudes 67°–125°W), and is consistent with the domain and resolution of the Land Data Assimilation System (LDAS)–North America project (see Mitchell et al. 1999). By construct, the surface energy and water budgets close

at each time step; no assimilation of land surface state observations is performed.

2. Hydrologic model description

The hydrologic model used in this study is the variable infiltration capacity (VIC) model (Liang et al. 1994, 1996). VIC is a macroscale hydrologic model that balances both surface energy and water over a grid mesh, typically at resolutions ranging from a fraction of a degree to several degrees latitude by longitude. Macroscale in this context refers to areas above a critical scale at which subgrid hydrologic variability can be captured statistically (e.g., Wood et al. 1988)—typically taken to be around 10 km. The controls of vegetation on land–atmosphere moisture and energy fluxes within VIC can be considered to constitute a soil–vegetation–atmosphere transfer scheme (SVAT). One distinguishing characteristic of the VIC model is its use of a subgrid parameterization of the effects of spatial variability in soils, topography, and vegetation that allows it to represent the observed nonlinear soil moisture dependence of the partitioning of precipitation into direct runoff and infiltration. It also features a nonlinear mechanism for simulating slow (baseflow) runoff response, and explicit treatment of vegetation effects on the surface energy balance.

In contrast with most SVATs, the VIC model generally [based, for example, on results of the Project for Intercomparison of Land Surface Parameterization Schemes (PILPS) experiments; Lohmann et al. 1998a] does a better job of reproducing observed runoff characteristics, whereas compared with other hydrologic models, it includes a full energy balance formulation absent from most hydrologic, or rainfall-runoff models. The VIC model has been successfully applied to many large global rivers (e.g., Abdulla et al. 1996; Lohmann et al. 1998b; Nijssen et al. 1997; Wood et al. 1997; Nijssen et al. 2001). For this study, the model was run at a ⅛° resolution from January 1950 through July 2000 (with 1949 used for a 1-yr spinup to remove the effects of initial moisture storages).

Prior to conducting the archived simulations described in section 5, simulations of more limited length were conducted for subareas of the domain shown in Fig. 1. The simulated runoff was routed through the grid cell network to strategic outlet points, where it was compared to observed, or, where available naturalized (water management effects removed) runoff. The simulated runoff was calibrated by adjustment of soil parameters describing soil depth, baseflow drainage and infiltration capacity of the soil layers, which is described in greater detail by Maurer et al. (2001), with the resulting "pseudo-observations" used to compare various coupled models.

1 Northwest   6 Missouri   11 Lower Mississippi
2 California   7 Arkansas-Red   12 Ohio
3 Great Basin   8 Gulf   13 East Coast
4 Colorado   9 Great Lakes   14 Canada
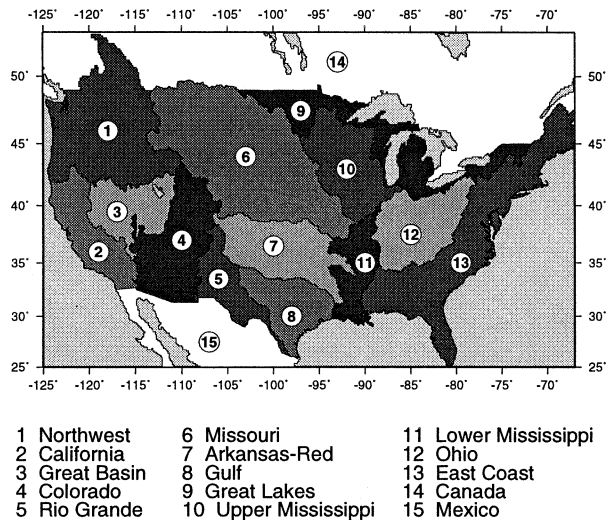5 Rio Grande   10 Upper Mississippi 15 Mexico

FIG. 1. LDAS domain with modeling subareas.

3. Model input datasets

a. Land surface characteristics

The soil characteristics used were taken from gridded ⅛° datasets developed as part of the LDAS (Mitchell et al. 1999) project. Within the conterminous United States, these datasets are based on the 1-km-resolution dataset produced by the Pennsylvania State University (Miller and White 1998). For areas in Canada and Mexico, the LDAS soil data are derived from the 5-min Food and Agriculture Organization dataset (FAO 1998). Soil texture in the LDAS dataset is divided into 16 classes for each of 11 layers, inferring specific soil characteristics (e.g., field capacity, wilting point, saturated hydraulic conductivity) based on the work of Cosby et al. (1984) and Rawls et al. (1998), and Reynolds et al. (2000). These LDAS datasets were used to specify the relevant soil parameters required by the VIC model directly. For remaining soil characteristics (e.g., soil quartz content), values were specified using the soil textures from the 1-km database, which were then indexed to published parameter values [the primary source was Rawls et al. (1993)], and aggregated to the ⅛° model resolution. The VIC model as applied in this study uses a three-layer soil column, with depths of each layer specified for each grid cell as derived during subarea calibration.

Land cover characterization was based on the University of Maryland global vegetation classifications described by Hansen et al. (2000), which has a spatial resolution of 1 km, and a total of 14 different land cover classes. From these global data we identified the land cover types present in each ⅛° grid cell in the model domain and the proportion of the grid cell occupied by each, as described by Maurer et al. (2001). The primary characteristic of the land cover that affects the hydrologic fluxes simulated by the VIC model is leaf area

index (LAI). LAI is derived from the gridded (¼°) monthly global LAI database of Myneni et al. (1997), which is inverted using the Hansen et al. land cover classification to derive monthly mean LAIs for each vegetation class for each grid cell. The LAI values do not change from year to year in this implementation of VIC; hence, interannual variations in vegetation characteristics are ignored. Furthermore, the Myneni et al. LAI values to which the method is tied are based on averages over the period 1981–94, which may not be representative of the entire simulation period. Rooting depth is specified for each land use type so that shorter crops and grasses draw moisture from the upper soil layers, and tree roots from the deeper layer (e.g., Jackson et al. 1996). Additional parameters for each vegetation type were assembled based on several sources, including roughness length and displacement height (Calder 1993), architectural resistance (Ducoudré et al. 1993), and minimum stomatal resistance (DeFries and Townshend 1994).

b. Meteorological and radiative forcings

The VIC model is forced with observed surface meteorological data which include precipitation, temperature, wind, vapor pressure, incoming longwave and shortwave radiation, and air pressure. Because only temperature and precipitation are measured routinely at a reasonably large number of locations within the domain, we use established relationships relating these other meteorological and radiation variables (excluding wind) to precipitation, daily temperature, and temperature range. For example, dewpoint temperature is calculated using the method of Kimball et al. (1997), which relates the dewpoint to the daily minimum temperature and precipitation, and downward shortwave radiation is calculated based on daily temperature range and dewpoint temperature using a method described by Thornton and Running (1999). Because surface observations of wind speed are sparse and are biased toward certain geographical settings (e.g., airports), daily 10-m wind fields were obtained from the NCEP–NCAR reanalysis (Kalnay et al. 1996), and regridded from the T62 Gaussian grid (approximately 1.9° square) to the ⅛° grid using linear interpolation.

Within the conterminous United States, precipitation data consist of daily totals from the National Oceanic and Atmospheric Administration (NOAA) Cooperative Observer (Co-op) stations, the average density of which is about one station per 700 km². Daily precipitation totals were assigned to each day based on the time of observation for the gauge. For example, a gauge reporting precipitation accumulation at 0700 local standard time would have 7/24 of the daily total assigned to the reporting day, and the remainder to the previous day. The precipitation gauge data were gridded to the ⅛° resolution using the synergraphic mapping system (SYMAP) algorithm of Shepard (1984) as implemented

by Widmann and Bretherton (2000). The gridded daily precipitation data were then scaled to match the long-term average of the parameter-elevation regressions on independent slopes model (PRISM) precipitation climatology (Daly et al. 1994, 1997), which is a comprehensive dataset of 12 monthly means for 1961–90 that is statistically adjusted to capture local variations due to complex terrain. This was done by generating 12 scale factors for each grid cell, one for each month, where each scale factor was the ratio of the PRISM mean monthly precipitation for 1961–90 to the mean monthly gridded, unscaled Co-op station precipitation for 1961–90. Although the PRISM data do account for the lower station density in more complex terrain, they do not include an adjustment for precipitation gauge under-catch, which can be significant especially for snowfall measurements (Goodison et al. 1998). For this reason, some underestimate of precipitation may still be present in snow-dominated areas. The minimum and maximum daily temperature data, also obtained from Co-op stations (approximately one station per 1000 square kilometers on average), were gridded using the same algorithm as for precipitation, and were lapsed (at $-6.5°C$ km^{-1}) to the grid cell mean elevation. Temperatures at each time step were interpolated by fitting an asymmetric spline through the daily maxima and minima.

For Canadian portions of the study area, the daily gridded precipitation and temperature data are generally of lower quality than in the U.S. part of the domain, due to lower station density and the need to include some less reliable sources to obtain a complete record. For the years 1949–99 (excluding British Columbia for 1999), observed daily temperature and precipitation station data (Environment Canada 1999) were used in the same manner as were such observations over the United States. Precipitation is measured at more than 2500 Environment Canada meteorological stations, resulting in an average station density of one station per 4000 square kilometers in the region of Canada included in this study (Metcalf et al. 1997). Additional sources of data were used to complete the precipitation and temperature forcings for British Columbia for 1999 and for all of Canada for 2000. For precipitation, the Global Precipitation Climatology Project (GPCP) gridded 1° precipitation product (Huffman et al. 2001) was used. The GPCP daily product, available from 1997 on, is derived from gauge data merged with satellite estimates of precipitation. The gauge data in the GPCP product include monthly precipitation reported via the World Weather Watch Global Telecommunication System, which are observations at a lower station density than the Environment Canada meteorological stations. For temperature, the NCEP–NCAR reanalysis product (Kalnay et al. 1996) daily minimum and maximum 2-m air temperatures were used. At present, the PRISM data do not include Canada or Mexico, with the exception of the Canadian portion of the Columbia River basin; hence, no rescaling of precipitation was performed for the portions of Canada or Mexico without PRISM data.

As for the Canadian portions of the study area, the Mexican portion also has a relatively low station density, and uses data sources that are generally less reliable than those used within the United States to obtain a complete record. For the years 1949–97, observed daily temperature and precipitation station data were used. Daily precipitation and temperature measurements were available from 1949 to 1997 at 132 stations in the Mexican region of the domain (Servicio Meteorológico Nacional 2000), for an average station density of one station per 6000 square kilometers. For 1998–2000, the GPCP precipitation and the NCEP–NCAR reanalysis air temperatures were used.

Daily precipitation totals were apportioned evenly over each 3-h, model time step. To evaluate the sensitivity of the diurnal cycle of model-predicted fluxes to this assumption, we developed a simple algorithm for disaggregating daily precipitation. From the NOAA/National Climatic Data Center (NOAA/NCDC) Co-op stations reporting hourly data, we derived the probabilities of time of occurrence and number of hours of precipitation, and created cumulative distribution functions of these for each season for five ranges of daily total precipitation at each Co-op station. Using these relationships, we stochastically disaggregated the gridded daily precipitation and ran the VIC model, with both disaggregated and nondisaggregated (evenly distributed through the day) daily precipitation. A comparison of the mean diurnal cycle of precipitation, runoff, and evapotranspiration from these two simulations, run over the lower Mississippi River basin for 1996–99, is shown in Fig. 2. Even in the summer, when the diurnal cycle of precipitation is strongest, the assumption of a uniform diurnal precipitation rate does not substantially affect the mean diurnal cycle of the partitioning of precipitation into evapotranspiration and runoff. The same is true for the mean diurnal cycle of the energy balance. The use of a constant daily precipitation rate does result in slightly increased runoff and decreased evapotranspiration. However, it should be noted that the model parameters were estimated based on a constant diurnal cycle of precipitation, and the results for disaggregated precipitation may be slightly biased as the model was not recalibrated to the disaggregated precipitation. Nonetheless, the results show that the assumption of a constant diurnal cycle has minimal effect on the model-derived moisture and energy fluxes.

4. Preliminary analysis

The parameterized forcings and model-simulated variables were compared to selected sets of observations, where available, in order to evaluate the quality of the model-simulated data. We present five comparisons here, both to confirm the validity of the derived variables, and to illustrate some potential uses of the dataset.
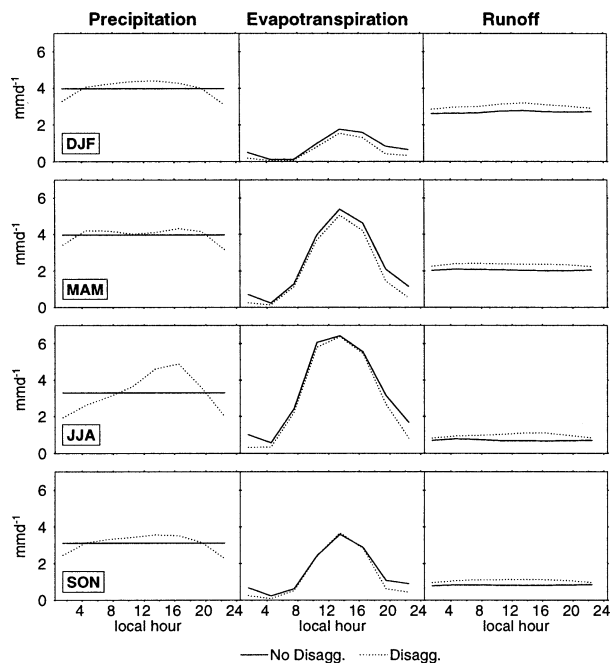
FIG. 2. Comparison of effect of stochastic disaggregation of daily precipitation totals vs constant precipitation rate on simulated runoff and evapotranspiration. Columns are for different variables, and rows are for each of the four seasons.

a. Comparison of routed VIC runoff with observed streamflow

As in previous applications of the VIC model, the runoff was routed from individual grid cells, through a defined channel network, to produce hydrographs at selected points. The routing algorithm is based on Lohmann et al. (1996), which uses daily runoff at each contributing grid cell. Although the routing model can be calibrated to improve timing of hydrographs, we performed no calibration of the routing model for this comparison. The resulting predicted hydrographs for 12 locations throughout the domain are shown in Fig. 3. For comparison, observed flows at U.S. Geological Survey (USGS) stream gauges are shown. In the case of the Columbia, Sacramento, Tuolumne, Colorado, Missouri, Alabama, and Potomac Rivers, naturalized flows, that is, observed flows that have been adjusted for anthropogenic effects (e.g., irrigation diversions, reservoir storage, and evaporation) are shown. In general, the VIC model is quite successful in capturing the peak flows, the baseflow-dominated low flows, and the interannual variation of streamflows.

Figure 4 shows the average annual cycle of the simulated and observed flows for the 10-yr time series in Fig. 3. As with Fig. 3, the range of flows represented varies widely between basins. The root-mean-square error (rmse) and relative bias for these 12 locations are summarized in Table 1. It should be noted that for the Arkansas River, significant withdrawals and diversions affect the observed flows, but unfortunately naturalized

flows for this river are not available for the period analyzed. Therefore it is expected that the simulated flows, which do not consider water management effects and diversions, will exceed the observed flows, and in fact the VIC simulations generally exceed the USGS observations. Based on data for 1995 (Solley et al. 1998), the depletions are estimated to be 10%–15% of the annual flow; thus, the relative bias in Table 1 would be reduced accordingly, as would the rmse. The bias over all areas, weighted by flow, is quite low; relative bias for the basins contributing the smallest amounts of flow tend to be larger than for the higher flow producing regions. The rmse, representing the average error in monthly flow simulation, shows the same pattern where rmse tends to be smaller for the areas contributing greater flows. The Moose River in Ontario, Canada, shows the highest bias and rmse of the basins included in Table 1. This reflects the lower density of meteorological stations in Canada; hence, greater uncertainty in the forcing data for the hydrologic model. In addition, the undercatch of frozen precipitation, which is not corrected for in this study, would be more important at higher latitudes. Further, no calibration to streamflow was performed for the portions of the domain in Canada (except the Canadian portion of the Columbia River basin, which was calibrated) or Mexico, for which soil parameters were transferred from the nearest calibrated basins in the United States. For the Columbia River basin, the rmse value is inflated due to the timing shift apparent in both Figs. 3 and 4, which illustrates the sensitivity of the rmse statistic when applied to timing errors in seasonal hydrographs. Although no calibration of the routing model was performed for this study, manually shifting the flows by 2 to 3 weeks reduces the rmse by 50%. This shows that the simulated model output, when used with a customized routing for each basin, could produce simulated streamflows with lower rmse than that shown in Table 1, although the bias would remain unchanged. It should be emphasized that the rmse values shown in Table 1 are applicable to individual months and years; the errors associated with mean flows averaged over n years would scale by approximately $1/n^{1/2}$.

Figure 5 illustrates three important characteristics of the simulated and observed monthly time series for each basin, using a Taylor diagram (Taylor 2001). The numbers plotted correspond to the numbering of the basins in Figs. 3 and 4, and the font size for each number is scaled by the cube root of the observed average flow. The radial distance from the origin to each number represents the ratio of the simulated to the observed standard deviation; the cosine of the azimuth angle represents the correlation of simulated streamflows with observations (after removal of the mean); and the distance from the point where observations would plot, located at (1, 0), is proportional to the rmse. Figure 5 shows good correlation of simulated and observed flows, with all basins exceeding 0.8, and most above 0.9. The most prominent feature is that the basins with the largest run-
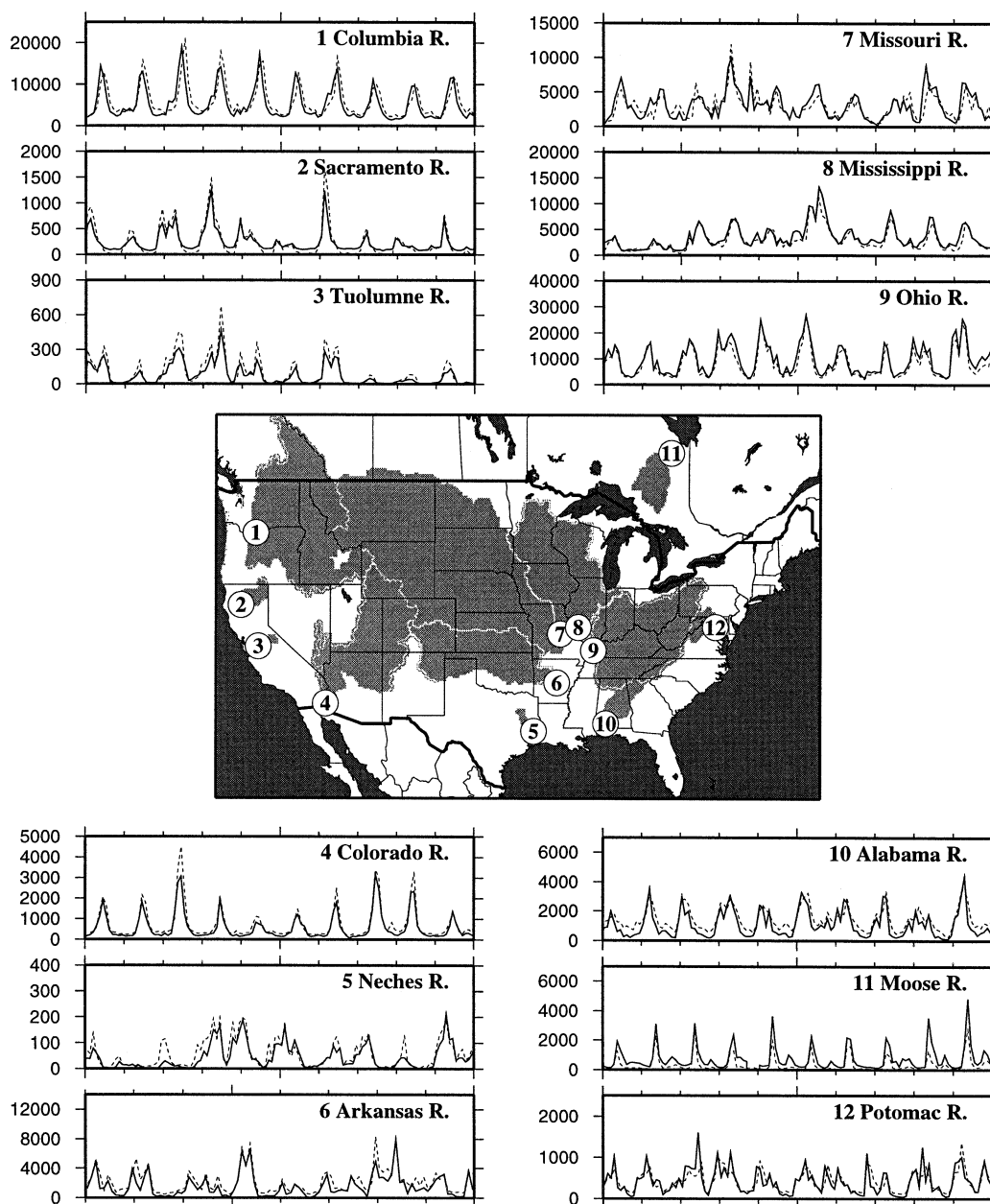
FIG. 3. Comparison of routed simulated runoff (dashed lines) with observed (or naturalized) streamflows (solid lines). Ordinate values are runoff in m³ s⁻¹, abcissa is a 10-yr period, the beginning of which varies by basin, depending on observed flow availability. Shaded areas in center panel are the contributing regions to each identified point.

off show the best correspondence with observed variance, plotting very close to the dashed line at the radial value of unity.

The overall success at reproducing runoff hydrographs, taken together with the use of observed precipitation, implies that, over timescales long enough for the change in surface storage to be small relative to the accumulated values for other variables in the water budget, evapotranspiration (ET) is realistically estimated. In addition, due to the physically based representation of soil moisture and runoff generation processes within the model, simulations of other surface flux and state variables (e.g., ET, total soil moisture storage, and snow) should reasonably represent the true (but unobserved) variables. Although runoff can be validated against observed streamflow at many locations, validation of other model-simulated variables, such as ET and soil moisture are more difficult due to the paucity of long-term observations over broad spatial domains. Ongoing validation of the dataset presented here will identify areas
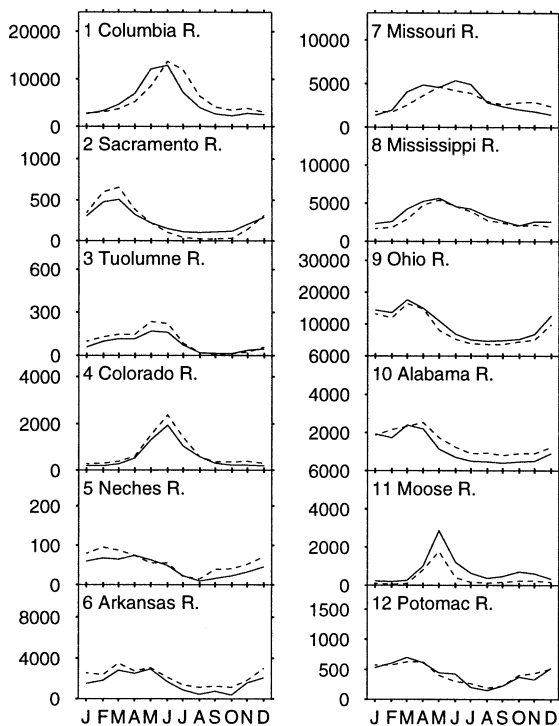
FIG. 4. Average flows by month for each of the 12 basins shown in Fig. 3. Ordinate values are m³ s⁻¹, solid lines are observed or naturalized flows, and dashed lines are routed simulated runoff.

TABLE 1. Simulated and observed streamflow comparison statistics.

River	Rmse* (%)	Relative bias** (%)	Avg obs flow (m³ s⁻¹)
Columbia	44.0	9.0	5349
Sacramento	46.4	− 0.4	239
Tuolumne	68.4	30.3	76
Colorado	45.7	26.7	580
Neches	61.4	29.5	44
Arkansas	56.3	35.0	1605
Missouri	38.8	−3.7	3119
Upper Mississippi	25.6	−13.8	3511
Ohio	21.3	−14.8	9760
Alabama	48.2	31.7	1113
Moose	71.8	−50.9	738
Potomac	47.9	0.5	424
Overall (weighted by obs. flow)	34.5	−3.1	

* Rmse $= [1/n\sqrt{\sum_{i=1}^{n} (Q_{s,i} - Q_{o,i})^2}/\overline{Q_o}] \times 100\%$ where $Q_{s,i}$ and $Q_{o,i}$ symbolize simulated and observed monthly flow rates, respectively, for month i. The number of months, n, is 120 for all basins.
** Relative bias $= [(\overline{Q_s} - \overline{Q_o})/\overline{Q_o}] \times 100\%$.

same period. The climatological soil moisture level for the VIC simulation is low relative to the observations, but the average monthly flux, which affects the model's water balance, is simulated quite accurately (Fig. 6b). This suggests that, at least in the Illinois area, the VIC simulation produces soil moisture storage changes that are consistent with observations.

Additionally, a monthly time series of average soil moisture in the top 1 m was computed for both the Illinois observations and the VIC simulations. The coefficient of variation of each month, defined as the standard deviation divided by the mean, is a measure of the interannual variability of soil moisture. Figure 6c shows that the coefficient of variation for the VIC simulations

where this approach performs best, and where improvements will be most valuable for future investigations. We will report later comparisons for a few locations where long-term observations of variables other than runoff are available.

b. Comparison with Illinois soil moisture

There are few systematic measurements of soil moisture within the model domain that provide records of a length sufficient for comparison to the VIC model simulation. The soil moisture database described by Hollinger and Isard (1994), available from as early as 1981 through August 1996 through the Global Soil Moisture Data Bank (Robock et al. 2000), is unique in the length and detail of the measurements. Observations are available from 19 sites distributed more or less uniformly over Illinois. Soil moisture is reported at 11 different depths to a total of 2 m, with a sampling interval of approximately every 2 weeks on average (less frequently in the winter). For comparison with these 19-point measurements, we selected the 17 VIC ⅛° grid cells that contain all of the observation locations. In addition, because the soil depths in the VIC grid cells vary between 1.0 and 2.3 m, only the soil moisture from the top 1 m from both the observations and the VIC model were used in the comparisons. Figure 6a compares the observed monthly average soil moisture for the top 1 m for 1981–96 with the VIC model simulation for the
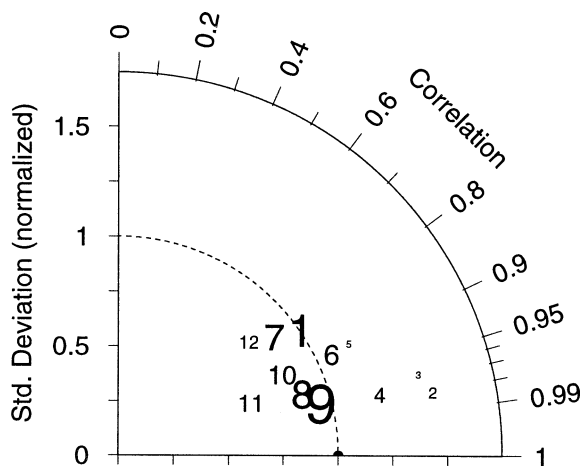

FIG. 5. Taylor diagram for simulated monthly runoff routed to basin outlet points. The plotted numbers identify the basin, using the same numbering system as used in Figs. 3 and 4, and are shown in font sizes scaled by the cube root of the observed flow. See text for details.
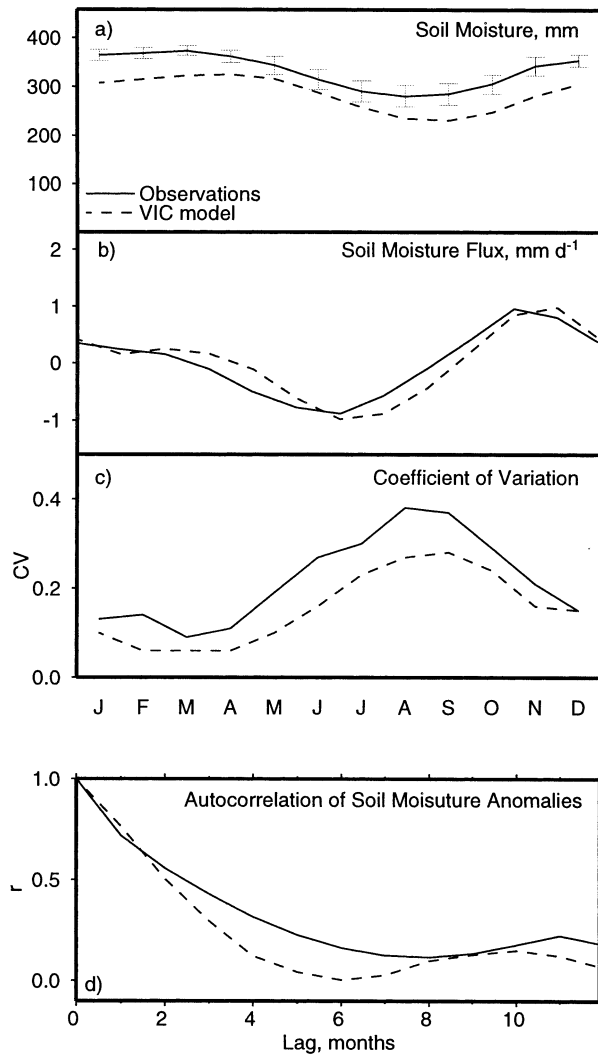
FIG. 6. Comparison of observed soil moisture (solid) in Illinois from 1981–96 with simulated values (dashed) for the same period. (a) Average soil moisture in the top 1-m of soil for each month; (b) average soil moisture tendency for each month; (c) coefficient of variation of monthly soil moisture anomalies; (d) autocorrelation of soil moisture anomalies.

slightly underestimates the seasonal variation of interannual variability seen in the observations. Finally, Fig. 6d illustrates that the autocorrelation of soil moisture anomalies in the VIC model is similar to that of observed data, which suggests that the persistence of soil moisture anomalies is comparable in the model and observations.

c. Comparison of diurnal cycle of surface fluxes with observations

To evaluate the simulated daily radiation, as well as the diurnal cycle, we use observations of selected sites in the continental United States established as part of the Surface Radiation Budget Network (SURFRAD;
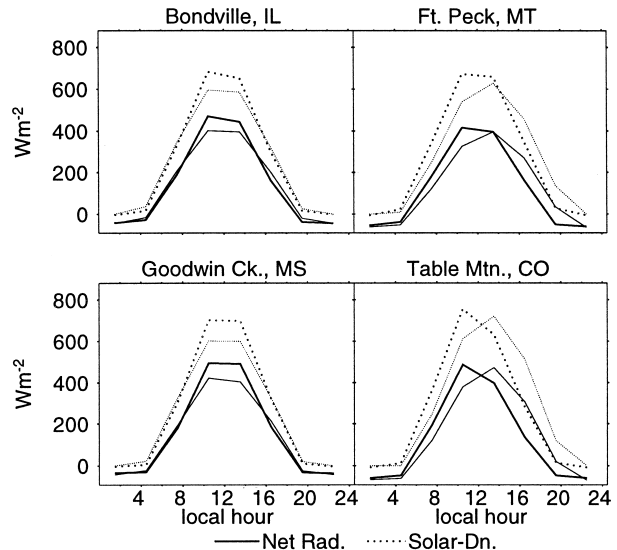

FIG. 7. Comparison of observed (thick lines) and simulated (thin lines) downward solar radiation (dotted) and net radiation (solid) at four SURFRAD sites. Data are averaged for Jun, Jul, and Aug, 1996–99, with the observations aggregated temporally to 3-h for comparison.

Augustine et al. 2000). We chose the four sites with the longest records, beginning in 1994–95, which are located in Mississippi, Montana, Illinois, and Colorado. Figure 7 shows the observed downward solar radiation and net (longwave plus shortwave) radiation fluxes at these four sites (aggregated from 3 min to 3 h, to match the VIC simulation time step), averaged for June, July, and August for 1996–99, and the model-simulated fluxes for the grid cells containing these points. Both the simulated average daily downward solar radiation and net radiation are within 10% of the observations at all locations; averaged over all sites, these are within 2%. There is a downward bias of the daily peak for these fluxes of between 3% and 15%, with an average of 10% over all sites. In general, the comparisons indicate reasonable agreement of daily radiative fluxes, with some peak radiation underestimation, across a wide range of geographical settings.

The First International Satellite Land Surface Climatology Project (ISLSCP) Field Experiment (FIFE) included an intensive collection of land surface flux data at multiple locations within a 15 km $\times$ 15 km site near Manhattan, Kansas, (centered at 39.05°N, 96.53°W). Intensive field campaigns were conducted during the summers of 1987 and 1989, generally of length about 2–3 weeks each, with continuing observations with fewer stations during the remainder of the summers, and during the summer of 1988 (Sellers et al. 1992). The resulting tower flux observations were compiled and quality controlled by Betts and Ball (1998). The dataset provides a multisite average of surface fluxes, reported every 30 min, that allows examination of the VIC model
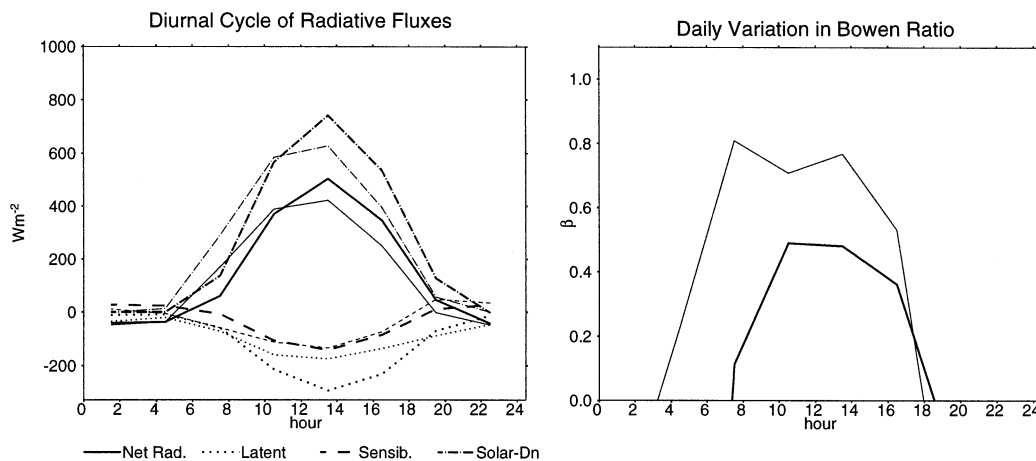
FIG. 8. Comparison of observed (thick lines) and simulated (thin lines) surface fluxes at the FIFE site using averaged Jun, Jul, and Aug values over 1987–89.

output with an observed diurnal cycle for surface flux variables.

As an example, we compare the average diurnal cycle of surface fluxes for the VIC grid cell centered at 39.0625°N, 96.5625°W, which is comparable to the FIFE site in location and dimension, measuring 13.9 km north–south × 10.8 km east–west. Figure 8a compares the average diurnal cycle for this grid cell with the FIFE observations for June–August, averaged over 1987–89. In general, the VIC-derived peak solar radiation is underestimated by 15%, while the daily average is underestimated by 7%. The net radiation is also underestimated relative to the observations, by 16% for the peak, and by 9% for the daily average. The average underestimate of the latent heat flux by VIC, for the averaged 1987–89 period, is 21 W m^{-2}, or 19%, which is equivalent to 0.73 mm day^{-1} of evaporation. This can be compared to estimates of the site-averaged nonclosure of the water balance for the observations, which for the period 29 May–16 October 1987 vary from 20 mm (Duan et al. 1996) to 40 mm (Betts and Ball 1998), or an average 0.14–0.28 mm day^{-1} over the observation period. As shown in Fig. 8b, the partitioning of the net radiation into latent and sensible heat does follow the pattern seen in the observations. The average simulated sensible heat flux exceeds the observed by 5 W m^{-2}, which is a 16% overestimation. The average Bowen ratio for daytime hours for the observations for this period is 0.36, and for VIC is 0.61. Although summer evapotranspiration for this grid cell shows some bias relative to the observations, since the model is forced with precipitation and reproduces observed runoff, evapotranspiration is correctly estimated over larger areas.

d. Derived soil moisture persistence

Huang et al. (1996) produced a 63-yr time series of monthly soil moisture for the conterminous United

States, using historical monthly average precipitation and temperature at 344 climate divisions. They developed a simple monthly water balance bucket-type soil model, where potential evapotranspiration was computed using a temperature index method, which was then scaled by the soil saturation level to estimate actual evapotranspiration. Surface runoff was calculated based on incident monthly precipitation, scaled by a nonlinear relation of saturation of the soil, and baseflow discharge from the soil column was a function of soil moisture in the column. Using their derived soil moistures, they produced maps of the autocorrelation of soil moisture, as well as correlations of soil moisture with precipitation and temperature. Huang et al. apply uniform soil model parameters to the conterminous United States, developed based on runoff data in Oklahoma and validated against soil moisture in Illinois. Figure 9 compares the autocorrelation of soil moisture anomalies at 3-, 6-, and 9-month lags for the VIC model output. Figure 9d is comparable to Fig. 3 in Huang et al. (1996). There is a strong correspondence with the VIC-derived statistics and Huang et al. (1996). For instance, both sets of results show higher soil moisture persistence toward the western portions of the domain, and more moderate levels in the north-central United States, though the VIC model correlations are generally lower than the Huang et al. values by 0.1 to 0.2. Focusing specifically on Illinois, at a 3-month lag the VIC model simulations show a monthly autocorrelation of soil moisture anomalies between May and August of approximately 0.25–0.3 (with an average of 0.28 over the Illinois area) while the Huang et al. model estimates approximately 0.35–0.5 for this region. By comparison, the Illinois soil moisture measurements show a 3-month autocorrelation of soil moisture anomalies for May–August of 0.27, again using the soil moisture observations discussed in section 4b. This suggests that, at least for Illinois, the more complex VIC model land surface representation reproduces observed soil moisture persistence somewhat bet-
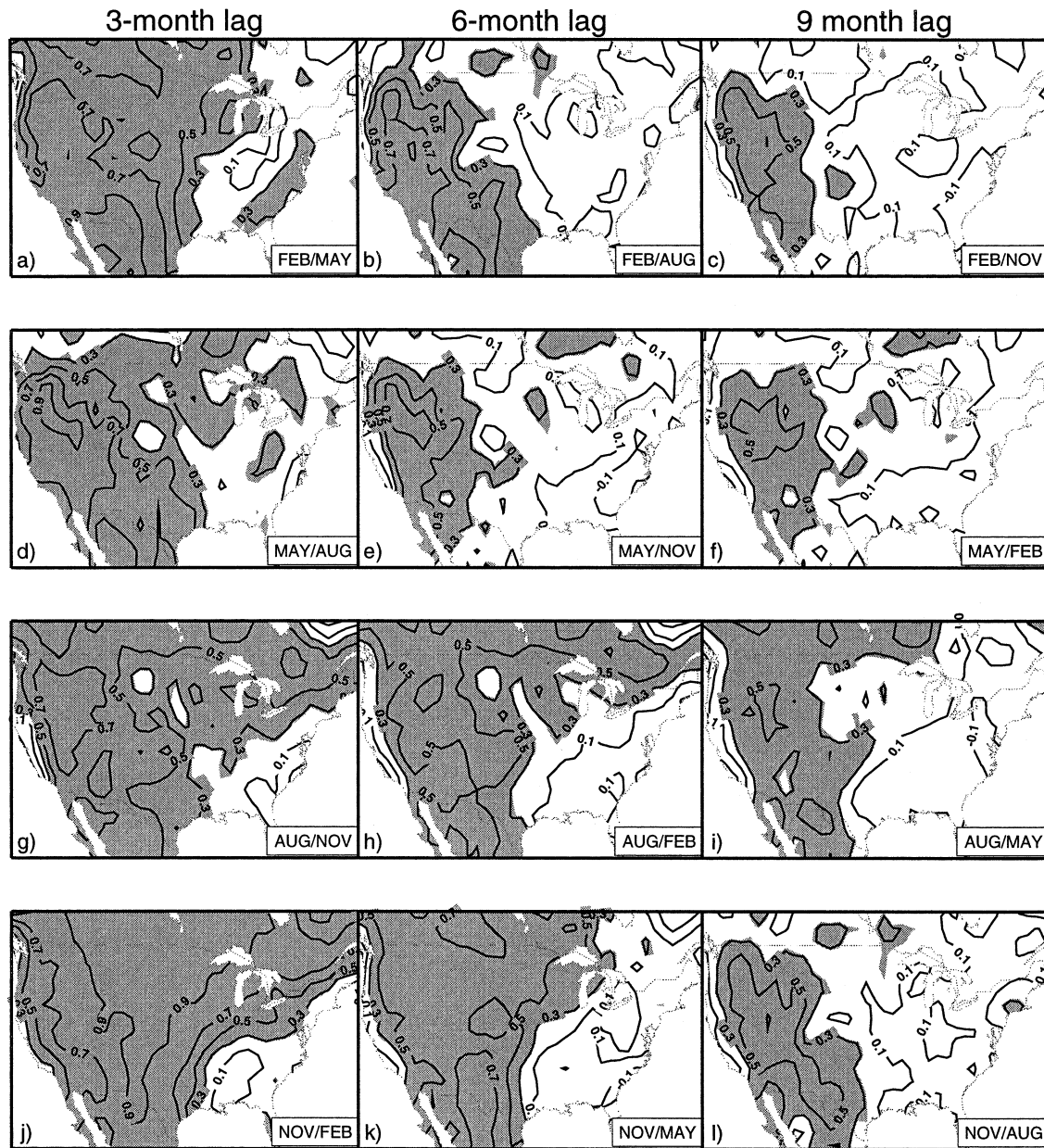
FIG. 9. Autocorrelation of soil moisture anomalies at lags of 3, 6, and 9 months. Shaded regions include correlations significant at a 0.05 level.

ter than does the more simplified model of Huang et al. Figure 9 also illustrates the decay of the autocorrelation with time. For instance, February soil moisture anomalies tend to dissipate more quickly than August anomalies, which have significant persistence over larger areas 9 months later.

e. Observed and simulated snow extent

Northern hemisphere snow-extent data are archived by the National Snow and Ice Data Center (1996) for the period 1971–95. These data were derived from dig-

itized versions of manual interpretations of Advanced Very High Resolution Radiometer (AVHRR), Geostationary Operational Environmental Satellite (GOES), and other visible band satellite data, and are gridded to a spatial resolution of 25 km. For comparison with the gridded observations of snow extent, Fig. 10 shows the areas that in the hydrologic model simulation, contain greater than 5 mm of snow water equivalent on the selected dates at least 80% of the time during 1971–95. The contour line in Fig. 10 shows for each date the extent to which snow cover is observed 80% of the time during the same period. It should be noted that there is
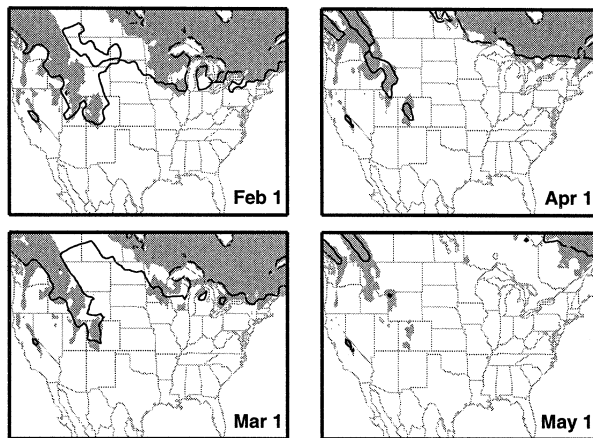
FIG. 10. Comparison of simulated snow water equivalent and the observed snow extent for 1971–95. Contour line indicates the extent of observed snow cover 80% of the time on the specified date. Shaded areas are those showing simulated snow water equivalent in excess of 5 mm 80% of the time on the indicated dates.

not direct, fixed correspondence between a specific snow water equivalent on the ground and snow extent detected by a satellite, but a qualitative assessment can be made on the basis of this comparison. Figure 10 illustrates three features of the model-simulated snow: the seasonal retreat of the snow line for the eastern half of the domain closely matches the observations; but the model underestimates snow extent in the northern Great Plains; and a slight overestimation of late-season snow by the model relative to the observations is apparent in some areas of the mountainous western United States. Cherkauer

(2001, his appendix A) in a study focused on the upper Mississippi River basin demonstrated the significant effect of correcting precipitation for undercatch of precipitation, especially frozen precipitation. The increase in winter (December, January, February) precipitation was greatest in northern areas, and may account for some of the difference in observed snow extent and simulated snow water equivalent in the northern Great Plains.

5. Data format and availability

The data described in this paper are archived in netCDF format. Monthly summaries of model forcing variables, model output, and derived variables are available to the public via FTP from our Web site (www.hydro.washington.edu). Arrangements are currently in progress to make the data set accessible via the University Corporation for Atmospheric Research (UCAR) Joint Office of Science Support. Details of access to the full dataset, which includes 3-h output and daily summary data archived by variable by year, are also available from our Web site. This site will also announce updates of the archive.

The variables included in the archive are listed in Table 2. For the 3-hourly data, flux variables (in units of either kg m^{-2} s^{-1} or W m^{-2}) reported at each time step are averages over the preceding 3 h. State variables (kg m^{-2}) are reported at the end of the time step. For monthly and daily summary data, both flux and state variables are averages of the eight reported values during that day. In addition to the model forcing and output

TABLE 2. Variables included in data archive.

	Variable name	Units
Variables (3-h and daily)		
Precipitation	Prate	kg m^{-2} s^{-1}
Evapotranspiration	Evap	kg m^{-2} s^{-1}
Runoff (surface)	Qs	kg m^{-2} s^{-1}
Baseflow	Qsb	kg m^{-2} s^{-1}
Soil moisture, layer 1	Soilm1	kg m^{-2}
Soil moisture, layer 2	Soilm2	kg m^{-2}
Soil moisture, layer 3	Soilm3	kg m^{-2}
Snow water equivalent	SWE	kg m^{-2}
Net shortwave radiation at the surface	SWnet	W m^{-2}
Incoming (downward) longwave radiation	LWdown	W m^{-2}
Net radiation at the surface	NetRad	W m^{-2}
Latent heat flux	Qle	W m^{-2}
Sensible heat flux	Qh	W m^{-2}
Ground heat flux	Qg	W m^{-2}
Albedo	Albedo	—
Surface (skin) temperature	RadT	K
Relative humidity	RH	%
Air temperature	Tair2	K
Wind speed	Wind	m s^{-1}
Variables (derived monthly)		
Average soil moisture tendency, layer 1	DelSoilm1	kg m^{-2} s^{-1}
Average soil moisture tendency, layer 2	DelSoilm2	kg m^{-2} s^{-1}
Average soil moisture tendency, layer 3	DelSoilm3	kg m^{-2} s^{-1}
Average snow water tendency	DelSWE	kg m^{-2} s^{-1}

variables, there are derived monthly summary data, including soil moisture and snow water fluxes averaged over each month. The variable names are generally consistent with the Assistance for Land Surface Modeling (ALMA) standards (Polcher et al. 2001). For variables not included in the ALMA list, variable naming conventions are based on the LDAS (Mitchell et al. 1999) common output standard.

6. Conclusions

We have described a derived dataset of land surface states and fluxes for the LDAS domain, which comprises the conterminous United States, and portions of Canada and Mexico. The dataset spans the period 1950–2000, and is at a resolution of ⅛°, or roughly 140 square kilometers per grid cell on average. The data are distinct from reanalysis products in that both the water and energy budgets at the land surface balance at every time step. Furthermore, the surface forcings include observed precipitation, and the simulated runoff is shown to match observations quite well over large river basins, indicating that, over the long term, in order to balance precipitation and runoff, evapotransporation must also be realistic. Given the physically based parameterizations in the model, we argue that over shorter timescales other terms in the surface water balance (e.g., soil moisture) are probably well represented, at least for the purposes of diagnostic studies such as those in which reanalysis products have been widely used. These characteristics give this dataset promise for proving useful for a variety of studies, especially where ground observations are lacking. As the data are extended through 2000 and 2001, the overlap of the dataset with archived model results including assimilation of remotely sensed observations will provide more opportunities for study.

REFERENCES

Abdulla, F. A., D. P. Lettenmaier, E. F. Wood, and J. A. Smith, 1996: Application of a macroscale hydrologic model to estimate the water balance of the Arkansas-Red River basin. *J. Geophys. Res.,* **101** (D3), 7449–7459.

Augustine, J. A., J. J. DeLuisi, and C. N. Long, 2000: SURFRAD—A national surface radiation budget network for atmospheric research. *Bull. Amer. Meteor. Soc.,* **81,** 2341–2357.

Beljaars, A. C., P. Viterbo, M. J. Miller, and A. K. Betts, 1996: The anomalous rainfall over the United States during July 1993: Sensitivity to land surface parameterization and soil moisture anomalies. *Mon. Wea. Rev.,* **124,** 362–383.

Betts, A. K., and J. H. Ball, 1998: FIFE surface climate and site-averaged dataset 1987–89. *J. Atmos. Sci.,* **55,** 1091–1108.

——, ——, A. C. M. Beljaars, M. J. Miller, and P. A. Viterbo, 1996a: The land surface–atmosphere interaction: A review based on observational and global modeling perspectives. *J. Geophys. Res.,* **101** (D3), 7209–7225.

——, S.-Y. Hong, and H.-L. Pan, 1996b: Comparison of NCEP–NCAR reanalysis with 1987 FIFE data. *Mon. Wea. Rev.,* **124,** 1480–1498.

Brubaker, K. L., D. Entekhabi, and P. S. Eagleson, 1993: Estimation of continental precipitation recycling. *J. Climate,* **6,** 1077–1089.

Calder, I. R., 1993: Hydrologic effects of land-use change. *Handbook of Hydrology,* D. R. Maidment, Ed., McGraw-Hill, 3.1–3.50.

Cherkauer, K. A., 2001: Understanding the hydrologic effects of frozen soil. Water Resources Series Tech. Rep. 167, University of Washington, Seattle, WA, 175 pp.

Coe, M. T., 2000: Modeling terrestrial hydrological systems at the continental scale: Testing the accuracy of an atmospheric GCM. *J. Climate,* **13,** 686–704.

Cosby, B. J., G. M. Hornberger, R. B. Clapp, and T. R. Ginn, 1984: A statistical exploration of the relationships of soil moisture characteristics to the physical properties of soils. *Water Resour. Res.,* **20,** 682–690.

Daly, C., R. P. Neilson, and D. L. Phillips, 1994: A statistical–topographic model for mapping climatological precipitation over mountainous terrain. *J. Appl. Meteor.,* **33,** 140–158.

——, G. H. Taylor, and W. P. Gibson, 1997: The PRISM approach to mapping precipitation and temperature. Preprints, *10th Conf. on Applied Climatology,* Reno, NV, Amer. Meteor. Soc., 10–12.

DeFries, R. S., and J. R. G. Townshend, 1994: NDVI-derived land cover classification at global scales. *Int. J. Remote Sens.,* **15,** 3567–3586.

Duan, Q. Y., J. C. Schaake, and V. I. Koren, 1996: FIFE 1987 water budget analysis. *J. Geophys. Res.,* **101** (D3), 7197–7207.

Ducoudré, N. I., K. Laval, and A. Perrier, 1993: SECHIBA, a new set of parameterizations of the hydrologic exchanges at the land–atmosphere interface within the LMD atmospheric general circulation model. *J. Climate,* **6,** 248–273.

Ebisuzaki, W., M. Kanamitsu, J. Potter, and M. Fiorino, 1998: An overview of Reanalysis-2. *Proc. 23rd Climate Diagnostics and Prediction Workshop,* Miami, FL, National Oceanic and Atmospheric Administration and Climate Prediction Center, 119–120.

Environment Canada, 1999: *Canadian Daily Climate Data on CD-ROM.* Environment Canada, Meteorological Service of Canada, Downsview, Ontario.

FAO, 1998: Digital soil map of the world and derived soil properties. Land and Water Digital Media Series 1, Food and Agriculture Organization, CD-ROM.

Gates, L. W., 1992: AMIP: The Atmospheric Model Intercomparison Project. *Bull. Amer. Meteor. Soc.,* **73,** 1962–1970.

——, and Coauthors, 1999: An overview of the results of the Atmospheric Model Intercomparison Project (AMIP I). *Bull. Amer. Meteor. Soc.,* **80,** 29–55.

Gibson, J. K., P. Kallberg, S. Uppala, A. Hernandez, A. Nomura, and E. Serrano, 1997: ERA description. Reanalysis Project Report Series, Vol. 1, European Centre for Medium-Range Weather Forecasts, Reading, United Kingdom, 72 pp.

Goodison, B. E., P. Y. T. Louie, and D. Yang, 1998: WMO solid precipitation measurement intercomparison. Instruments and

Observing Methods Rep. 67 (WMO/TD 872), World Meteorological Organization, Geneva, Switzerland, 212 pp.

Hansen, M. C., R. S. DeFries, J. R. G. Townshend, and R. Sohlberg, 2000: Global land cover classification at 1 km spatial resolution using a classification tree approach. *Int. J. Remote Sens.,* **21,** 1331–1364.

Higgins, R. W., K. C. Mo, and S. D. Schubert, 1996: The moisture budget of the central United States as evaluated in the NCEP/NCAR and the NASA/DAO reanalyses. *Mon. Wea. Rev.,* **124,** 939–963.

Hollinger, S. E., and S. A. Isard, 1994: A soil moisture climatology of Illinois. *J. Climate,* **7,** 822–833.

Hornberger, G. M., and Coauthors, 2001: A plan for a new science initiative on the global water cycle. U.S. Global Change Research Program, Washington, DC, 118 pp.

Huang, J., H. M. Van den Dool, and K. P. Georgakakos, 1996: Analysis of model-calculated soil moisture over the United States (1931–1993) and applications to long-range temperature forecasts. *J. Climate,* **9,** 1350–1362.

Huffman, G. J., R. F. Adler, M. M. Morrissey, S. Curtis, R. Joyce, B. McGavock, and J. Susskind, 2001: Global precipitation at one-degree daily resolution from multi-satellite observations. *J. Hydrometeor.,* **2,** 36–50.

Jackson, R. B., J. Canadell, J. R. Ehringer, H. A. Mooney, O. E. Sala, and E. D. Schulze, 1996: A global analysis of root distributions for terrestrial biomes. *Oecologia,* **108,** 389–411.

Janowiak, J. E., A. Gruber, C. R. Kondragunta, R. E. Livezy, and G. J. Huffman, 1998: A comparison of the NCEP–NCAR reanalysis precipitation and the GPCP rain gauge–satellite combined dataset with observational error considerations. *J. Climate,* **11,** 2960–2979.

Kalnay, E., and Coauthors, 1996: The NCEP/NCAR 40-Year Reanalysis Project. *Bull. Amer. Meteor. Soc.,* **77,** 437–471.

Kanamitsu, M., W. Ebisuzaki, J. Woolen, J. Potter, and M. Fiorino, 2000: An overview of NCEP/DOE Reanalysis-2. *Proc. Second WCRP Int. Conf. on Reanalyses,* Reading, United Kingdom, World Climate Research Programme, Rep. WCRP 109, 1–4.

Kimball, J. S., S. W. Running, and R. Nemani, 1997: An improved method for estimating surface humidity from daily minimum temperature. *Agric. For. Meteor.,* **85,** 87–98.

Koster, R. D., T. Oki, and M. J. Suarez, 1999: The off-line validation of land surface models: Assessing success at the annual timescale. *J. Meteor. Soc. Japan,* **77B,** 257–263.

——, M. J. Suarez, and M. Heiser, 2000: Variance and predictability of precipitation at seasonal-to-interannual timescales. *J. Hydrometeor.,* **1,** 26–46.

Lenters, J. D., M. T. Coe, and J. A. Foley, 2000: Surface water balance of the continental United States, 1963–1995: Regional evaluation of a terrestrial biosphere model and the NCEP/NCAR reanalysis. *J. Geophys. Res.,* **105** (D17), 22 393–22 425.

Liang, X., D. P. Lettenmaier, E. Wood, and S. J. Burges, 1994: A simple hydrologically based model of land surface water and energy fluxes for general circulation models. *J. Geophys. Res.,* **99** (D7), 14 415–14 428.

——, ——, and ——, 1996: One-dimensional statistical dynamic representation of subgrid spatial variability of precipitation in the two-layer variable infiltration capacity model. *J. Geophys. Res.,* **101** (D16), 21 403–21 422.

Lohmann, D., R. Nolte-Holube, and E. Raschke, 1996: A large-scale horizontal routing model to be coupled to land surface parameterization schemes. *Tellus,* **48A,** 708–721.

——, and Coauthors, 1998a: The Project for Intercomparison of Land-surface Parameterization Schemes (PILPS) phase 2(c) Red-Arkansas basin experiment: 3. Spatial and temporal analysis of water fluxes. *Global Planet. Change,* **19,** 161–179.

——, E. Raschke, B. Nijssen, and D. P. Lettenmaier, 1998b: Regional scale hydrology. II. Application of the VIC-2L model to the Weser River, Germany. *Hydrol. Sci. J.,* **43,** 131–141.

Mahrt, L., and H. Pan, 1984: A two-layer model of soil hydrology. *Bound.-Layer Meteor.,* **29,** 1–20.

Manabe, S., 1969: Climate and the ocean circulation. I. The atmospheric circulation and the hydrology of the earth's surface. *Mon. Wea. Rev.,* **97,** 739–774.

Maurer, E. P., B. Nijssen, and D. P. Lettenmaier, 2000: Use of reanalysis land surface water budget variables in hydrologic studies. *GEWEX News,* **10** (4), 6–8.

——, G. M. O'Donnell, D. P. Lettenmaier, and J. O. Roads, 2001: Evaluation of the land surface water budget in NCEP/NCAR and NCEP/DOE reanalyses using an off-line hydrologic model. *J. Geophys. Res.,* **106** (D16), 17 841–17 862.

Metcalfe, J. R., B. Routledge, and K. Devine, 1997: Rainfall measurement in Canada: Changing observational methods and archive adjustment procedures. *J. Climate,* **10,** 92–101.

Miller, D. A., and R. A. White, 1998: A conterminous United States multilayer soil characteristics dataset for regional climate and hydrology modeling. *Earth Interactions,* **2**. [Available online at http://EarthInteractions.org.]

Mitchell, K., and Coauthors, 1999: The GCIP Land Data Assimilation (LDAS) Project—Now underway. *GEWEX News,* **9** (4), 3–6.

Myneni, R. B., R. R. Nemani, and S. W. Running, 1997: Estimation of global leaf area index and absorbed PAR using radiative transfer models. *IEEE Trans. Geosci. Remote Sens.,* **35,** 1380–1393.

Namias, J., 1952: The annual course of month-to-month persistence in climatic anomalies. *Bull. Amer. Meteor. Soc.,* **33,** 279–285.

——, 1962: Influences of abnormal heat sources and sinks on atmospheric behavior. *Proc. Int. Symp. on Numerical Weather Prediction,* Tokyo, Japan, Meteor. Soc. Japan, 615–627.

National Snow and Ice Data Center, 1996: *Northern Hemisphere Weekly Snow Cover and Sea Ice Extent.* Vol. 1.0 and 2.0, Cooperative Institute for Research in Environmental Studies, University of Colorado, Boulder, CO, CD-ROM.

Nijssen, B., D. P. Lettenmaier, X. Liang, S. W. Wetzel, and E. Wood, 1997: Streamflow simulation for continental-scale basins. *Water Resour. Res.,* **33,** 711–724.

——, G. M. O'Donnell, D. P. Lettenmaier, D. Lohmann, and E. F. Wood, 2001: Predicting the discharge of global rivers. *J. Climate,* **14,** 3307–3323.

Pitman, A. J., and Coauthors, 1999: Key results and implications from phase 1(c) of the Project for Intercomparison of Land-surface Parameterization Schemes. *Climate Dyn.,* **15,** 673–684.

Polcher, J., L. Bowling, and D. Lettenmaier, 2001: First use of ALMA in PILPS 2e. *GEWEX News,* **11** (3), 11–14.

Rawls, W. J., L. R. Ahuja, D. L. Brakensiek, and A. Shirmohammadi, 1993: Infiltration and soil water movement. *Handbook of Hydrology,* D. Maidment, Ed., McGraw-Hill, 5.1–5.51.

——, D. Gimenez, and R. Grossman, 1998: Use of soil texture, bulk density, and slope of the water retention curve to predict saturated hydraulic conductivity. *Trans. ASAE,* **41,** 983–988.

Reynolds, C. A., T. J. Jackson, and W. J. Rawls, 2000: Estimating soil water-holding capacities by linking the Food and Agriculture Organization soil map of the world with global pedon databases and continuous pedotransfer functions. *Water Resour. Res.,* **36,** 3653–3662.

Roads, J., and A. Betts, 2000: NCEP/NCAR and ECMWF reanalysis surface water and energy budgets for the Mississippi River basin. *J. Hydrometeor.,* **1,** 88–94.

Robock, A., C. A. Schlosser, K. Y. Vinnikov, N. A. Speranskaya, J. K. Entin, and S. Qiu, 1998: Evaluation of the AMIP soil moisture simulations. *Global Planet. Change,* **19,** 181–208.

——, K. Y. Vinnikov, G. Srinivasan, J. K. Entkin, S. E. Hollinger, N. A. Speranskaya, S. Liu, and A. Namkhai, 2000: The global soil moisture data bank. *Bull. Amer. Meteor. Soc.,* **81,** 1281–1299.

Sellers, P. J., F. G. Hall, G. Asrar, D. E. Strebel, and R. E. Murphy, 1992: An overview of the first international satellite land surface climatology project (ISLSCP) field experiment (FIFE). *J. Geophys. Res.,* **97,** 18 345–18 371.

Servicio Meteorológico Nacional, 2000: Dat322 v. 1.0 (CD-ROM). Instituto Mexicano de Tecnología del Agua, Comisión Nacional del Agua, Morelos, México.

Shepard, D. S., 1984: Computer mapping: The SYMAP interpolation algorithm. *Spatial Statistics and Models,* G. L. Gaile and C. J. Willmott, Eds., D. Reidel, 133–145.

Solley, W. B., R. R. Pierce, and H. A. Perlman, 1998: Estimated use of water in the United States in 1995. U.S. Geological Survey Circular 1200, Denver, CO, 71 pp.

Taylor, K. E., 2001: Summarizing multiple aspects of model performance in a single diagram. *J. Geophys. Res.,* **106,** 7183–7192.

Thornton, P. E., and S. W. Running, 1999: An improved algorithm for estimating incident daily solar radiation from measurements of temperature, humidity, and precipitation. *Agric. For. Meteor.,* **93,** 211–228.

Trenberth, K. E., and C. J. Guillemot, 1998: Evaluation of the atmospheric moisture and hydrological cycle in the NCEP/NCAR reanalysis. *Climate Dyn.,* **14,** 213–231.

Widmann, M., and C. S. Bretherton, 2000: Validation of mesoscale precipitation in the NCEP reanalysis using a new gridcell dataset for the northwestern United States. *J. Climate,* **13,** 1936–1950.

Wood, E. F., M. Sivapalan, K. Beven, and L. Band, 1988: Effects of spatial variability and scale with implications to hydrologic modeling. *J. Hydrol.,* **102,** 29–47.

——, D. Lettenmaier, X. Liang, B. Nijssen, and S. W. Wetzel, 1997: Hydrological modeling of continental-scale basins. *Annu. Rev. Earth Planet. Sci.,* **25,** 279–300.

Xie, P., and P. A. Arkin, 1997: Global precipitation: A 17-year monthly analysis based on gauge observations, satellite estimates, and numerical model outputs. *Bull. Amer. Meteor. Soc.,* **78,** 2539–2558.

Ziegler, A. D., J. Sheffield, E. F. Wood, E. P. Maurer, B. Nijssen, and D. P. Lettenmaier, 2002: Detection of an acceleration in the global water cycle: The potential role of FRIEND. *FRIEND 2002—Regional Hydrology: Bridging the Gap between Research and Practice,* H. A. J. van Lanen and S. Demuth, Eds., IAHS Series of Proceedings and Reports, No. 274, International Association of Hydrological Sciences, 51–57.